Remediation of Crystal Violet Dye Aqueous Solution Using Agro Waste Based Activated Carbon: Equilibrium and Kinetics Studies

Chukwunonso Chukwuzuloke Okoye[1*], Okechukwu Dominic Onukwuli[1], Chinenye Faith Okey-Onyesolu[1] and Ifeoma Amaoge Obiora-Okafo[1]

[1]*Department of Chemical Engineering, Nnamdi Azikiwe University, P.M.B. 5025, Awka, Anambra State, Nigeria.*

Authors' contributions

This work was carried out in collaboration among all authors. Authors CCO and ODO designed the study, performed the statistical analysis, wrote the protocol and wrote the first draft of the manuscript. Authors CCO and CFOO managed the analyses of the study. Authors IAOO and CFOO managed the literature searches. All authors read and approved the final manuscript.

Article Information

Original Research Article

ABSTRACT

Remediation of crystal violet (CV) dye aqueous solution was attempted using acid activated *raphia hookeri* seeds (AARHS) as adsorbent. Adsorption equilibrium and kinetics of CV dye uptake onto AARHS were examined in series of experimental runs, and effects of contact time and initial CV dye concentrations were investigated at different solution temperatures (303 K, 313 K and 323 K). Equilibrium and kinetic data modeling of the adsorption process was performed using selected theoretical methods. Four different forms of Langmuir (type I, II, III and IV) and Freundlich isotherms were considered for fitting the equilibrium data while zero order, first order, pseudo-first order (PFO), second order, types I, II, III and IV pseudo-second order (PSO) and intra-particle diffusion models were selected to describe the kinetics of the adsorption process. Error functions including coefficient of determination (R^2), root mean square error (RMSE), chi square (χ^2) and average relative error (ARE) were employed to reveal model of best fit. Results obtained from error value computations show that the equilibrium data best followed Freundlich isotherm, which

---

Corresponding author: Email: cc.okoye@unizik.edu.ng, okoyecc7@gmail.com;

indicates multilayer adsorption of CV dye onto AARHS. The calculated Freundlich's adsorption intensity values at different temperatures reveal the favourability of the adsorption process. PSO type I, II and IV best fitted the kinetic data compared to other investigated models. Intra-particle diffusion plots depict that the adsorption process of CV dye onto AARHS is a two-step process and also, intra-particle diffusion is not the only rate-limiting step.

1. INTRODUCTION

Wastewaters emanating from textile, pulp and paper, pharmaceuticals, food processing industries among others emit coloured and toxic effluents to aquatic bodies rendering them unfit for human use. According to [1;2], greater numbers of these dyes are synthetic in nature and are usually composed of aromatics rings in their structure. Textile and dyeing industry are among important sources for the continuous pollution of the aquatic environment [3]. Dye-containing effluents display recalcitrant and non-biodegradable characteristics when discharged into aquatic bodies. These features suggest that dyeing waste effluent need to be treated before its discharge to the environment.

The undesirability of colour causing compounds in effluents is because they contain high levels of chemicals, suspended solids, and toxic compounds which are very detrimental to aquatic flora and fauna and cause many water borne diseases [3]. To protect the environment and water resources from negative effects, various treatment methods have been applied. The conventional methods of colour removal from industrial effluents include ion exchange, activated carbon adsorption, membrane technology and coagulation [4]. Among the numerous techniques designed for dye removal, adsorption is one of the best conventional treatment techniques, and has been considered for its low-cost, simplicity of design and easy availability of adsorbents, high efficiency, ease of operation and ability to treat dyes in more concentrated forms [5;6;7].

Research findings suggest the potentiality of adsorbents in final decolourization of pretreated wastewater or dye removal from rinsing waters for direct water recycling. The effectiveness of an adsorbent can be measured considering its (i) high affinity and capacity for target compounds, (ii) regeneration possibility (iii) safe and economically viable treatment/disposal of regenerate, (iv) tolerance for wide range of waste water parameters, and (v) usability for all or nearly all- reactive dyes [8]. Activated carbon is widely sorted after owing to its high adsorptive efficiency in water and wastewater treatment. The usage of activated carbon is limited by its high cost thus researches are geared toward investigating several low cost materials of regenerative resource to serve as alternative materials for treatment of dye-containing effluents. [9;10] divided these materials into three classes: inorganic materials, e.g., bentonite, gypsum, zeolite, and kaolin; industrial by-products, e.g., metal hydroxide sludge, sewage sludge, fly ash, and red mud; and agricultural solid waste, e.g., sawdust, chitosan, pine cones, rice husks, and coconut coir. This present study considered the use of *raphia hookeri seeds*, an agro waste, as a precursor for preparation of an adsorbent for the remediation of crystal violet aqueous solution.

In-depth understanding and proper interpretation of adsorption isotherms is vital for the overall improvement of adsorption mechanism pathways, effective design and optimization of adsorption systems [11;12;13]. Findings from adsorption kinetics study are significantly important in the design of an adsorption system because it supplies helpful information on the reaction pathway, rate of adsorption and mechanism of sorption [12;14].

This work aims at investigating the performance of an adsorbent derived from an agro waste, *raphia hookeri seeds,* for the remediation of crystal violet dye aqueous solution. The influence of contact time and solution temperature on amount of CV dye adsorbed was examined. Kinetics and equilibrium data modeling of the adsorption process was performed using selected theoretical methods.

2. MATERIALS AND METHODS

2.1 Adsorbate

The structure, maximum wavelength, molecular formula, molar mass and extinction coefficient of the adsorbate, CV dye, were presented in Table 1. A standard dye solution of 1000 mg/L was

prepared for CV dye by dissolving an appropriate quantity of CV dye in one litre of de-ionized water. Other required initial concentrations of dye solutions were prepared by proper dilution of the standard solution. 0.1 M HCl and 0.1 M NaOH stock solutions were used as pH adjusters of the working solutions to desired values. CV dye and other chemicals of analytical grades were purchased from a chemical vendor at Bridge Head Onitsha, Anambra State, Nigeria and used without further purification.

2.2 Adsorbent

The adsorbent was prepared according to the method earlier reported in Okoye et al., [15]. The precursor for the adsorbent preparation, *raphia hookeri* seeds, was sourced from south eastern part of Nigeria. *Raphia hookeri* seeds (RHS) were collected from Amasiri in Ebonyi state. RHS was properly washed to remove unwanted materials, sand, dirt, etc. The washed sample was air dried for 6 hours, and then oven dried for 4 hours at temperature of 383 K. The dried RHS sample size was reduced to 1 – 3mm and carbonized at 1173 K for 3 hours in a muffle furnace. The carbonized sample was soaked in 60% by weight hydrochloric acid (HCl) for 24 hours at impregnation (activating agent to carbonized sample) ratio of 1:1 weight basis. The resulting carbon was washed until the value of the leachate's pH ranged between 6 and 8, then dried in an oven at a temperature of 378 K for 5-6 hours. The activated carbon (AARHS) was cooled to room temperature in a desiccator. The resultant sample size was reduced and stored in properly labeled air tight container for further experiments.

2.2.1 Adsorbent characterization

Physic-chemical characterization of the sample was done. The measured properties include: surface area, percentage ash content, moisture content, bulk density and pH.

The functional groups present in AARHS were determined using FTIR spectrometer (Shimadzu FTIR 8400) over a range of 4000 – 400 cm^{-1} while the micrographs of the scanning electron microscope (SEM) was used to reveal the surface morphology of the activated carbon (AARHS).

2.3 Adsorption Study

A known mass of AARHS was mixed with 100 ml of aqueous CV dye solution of known concentrations in series of 250 ml Pyrex glass beakers placed on magnetic stirrers with hot plates and stirred at 110 rpm for predetermined residence times. 0.1 M HCl and 0.1 M NaOH stock solutions were employed as pH adjusters to desired pH value. The batch equilibrium experiments were conducted at adsorbate concentration of 100 mg/L, 1 g adsorbent dosage, pH 2, 75 µm adsorbent particle size and temperatures 303 K, 313 K, and 323 K. The experimental procedure was repeated for 150, 200, 300 and 500 mg/L adsorbate concentrations. Kinetic experiments were also conducted under similar conditions stated for equilibrium experiments at varying times (10 – 150 minutes) and solution temperatures (303 K, 313 K, and 323 K). At predetermined times, aliquots were withdrawn from the beakers and filtered using Whatman No. 1 filter paper. Dye concentration in the filtered sample was measured using a visible spectrophotometer. The amount of dye adsorbed was calculated from equation 1:
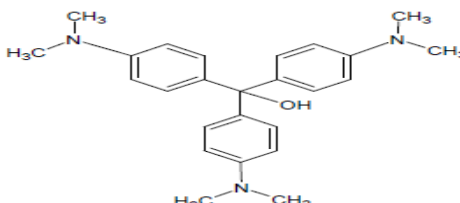
$$q_e = \frac{(C_o - C_e)V}{m} \tag{1}$$

Where C_o and C_e, the dye concentration (mg/L) at the initial time and at a time t, respectively, m defines the mass of the adsorbent (g) and V, the volume of adsorbate (L).

2.3.1 Isotherm models

Adsorption is usually described through isotherms, which explains the relation of the amount of adsorbate on the adsorbent as a function of its pressure -gas- or concentration -liquid- at constant temperature [16]. In this study, the equilibrium data was fitted into the linear forms of two isotherm models, namely: Langmuir and Freundlich isotherm models. Langmuir isotherm model was linearized and rearranged into four different types as shown in Table 2. The Langmuir's model constants were obtained by plotting Ce/qe vs Ce, 1/qe vs 1/Ce, qe vs qe/Ce and qe/Ce vs qe (equations 2, 3, 4 and 5) for type I, II, III, and IV respectively, also, from the plot of lnqe vs lnCe (equation 6), Freundlich's model constants were derived. Langmuir's maximum monolayer coverage capacity (qm) and constant related to the energy of adsorption (KL) for types I, II, III and IV; Freundlich's degree of nonlinearity between solution concentration and adsorption (n) and isotherm constant (KF) were calculated from the slopes and intercepts of Figs. S1, S2, S3, S4 and S5 respectively (supplementary data).

Table 1. Physical properties and molecular structure of CV

Properties	Nomenclature
Dye name	Crystal violet
IUPAC name	Tris(4-(dimethylamino)phenyl)methylium chloride
Molecular formula	$C_{25}H_{30}ClN_3$
Max. absorbance wavelength (λ_{max})	590 nm
Molar mass	407.99 $gmol^{-1}$
Extinction coefficient	87,000 $M^{-1}cm^{-1}$
Molecular structure	

Table 2. Isotherms and their expressions

Isotherm	Nonlinear	Linear	Plot	Parameters	Eqn no.	Ref
Langmuir-I	$q_e = \dfrac{q_m K_L C_e}{1 + K_L C_e}$	$\dfrac{C_e}{q_e} = \dfrac{C_e}{q_m} + \dfrac{1}{K_L q_m}$	$\dfrac{C_e}{q_e} vs C_e$	K_L= slope/intercept , q_m=slope^{-1}	2	[17]
Langmuir-II		$\dfrac{1}{q_e} = \left(\dfrac{1}{K_L q_m}\right)\dfrac{1}{C_e} + \dfrac{1}{q_m}$	$\dfrac{1}{q_e} vs \dfrac{1}{C_e}$	K_L= intercept/slope, q_m=intercept^{-1}	3	
Langmuir-III		$q_e = q_m - \left(\dfrac{1}{K_L}\right)\dfrac{q_e}{C_e}$	$q_e vs \dfrac{q_e}{C_e}$	K_L= -slope^{-1}, q_m=intercept	4	
Langmuir-IV		$\dfrac{q_e}{C_e} = K_L q_m - K_L q_e$	$\dfrac{q_e}{C_e} vs q_e$	K_L=-slope, q_m=-(intercept/slope)	5	
Freundlich	$q_e = K_F C_e^{\frac{1}{n}}$	$\ln q_e = \ln K_F + \dfrac{1}{n} C_e$	$\ln q_e vs \ln C_e$	K_F=exp(intercept), 1/n=slope	6	[18]

Langmuir isotherm quantitatively describes the formation of a monolayer adsorbate on the outer surface of the adsorbent, and after that no further adsorption takes place. This, therefore, suggests that the validity of Langmuir isotherm covers only for monolayer surface adsorption mechanism with fixed number of adsorption sites [17;19;20]. Freundlich isotherm is an empirical relationship which defines adsorption processes that occur on heterogeneous surfaces. The isotherm explains the surface heterogeneity and exponential distribution of active sites and their energies [13;19].

2.3.2 Adsorption kinetics models

Table 3 displays the mathematical expressions for the investigated kinetic models. The parameters of the zero order, first order, PFO, second order, PSO type I, II, III and IV; and intra-particle diffusion models were obtained from the linearized plots of q_t vs t, ln q_t vs t, ln(q_e-q_t) vs t, 1/q_t vs t, t/q_t vs t, 1/q_t vs 1/t, q_t vs q_t/t, q_t/t vs q_t and q_t vs $t^{1/2}$.

2.4 Validity of Models

The suitability of the isotherms in fitting the equilibrium data and the capability of the investigated kinetic models in describing the kinetic behavior of the adsorptive system, apart from the coefficient of determination (R^2) were further validated using root mean square error (RMSE), chi square (χ^2) and average relative error (ARE). These error functions can be expressed as:

$$RMSE = \sqrt{\frac{1}{N}\sum_{i=1}^{n}\left(\frac{q_{exp} - q_{cal}}{q_{exp}}\right)^2} \qquad (16)$$

$$\chi^2 = \sum_{i=1}^{n}\frac{(y_{i,p} - y_{i,e})^2}{y_{i,p}} \qquad (17)$$

$$ARE\ (\%) = \frac{100}{N}\sum_{i=1}^{N}\left|\frac{q_{exp} - q_{calc}}{q_{exp}}\right| \qquad (18)$$

Table 3. Kinetic models and their expressions

Kinetic models	Nonlinear	Linear	Plot	Parameters	Eqn no.	Ref
Zero order	$q_t = q_e - k_0 t$	$q_t = q_e - k_0 t$	$q_t\ vs\ t$	k_0 = -slope, qe = intercept	7	
First order	$q_e = q_t \exp(k_1 t)$	$\ln q_t = \ln q_e - k_1 t$	$\ln q_t\ vs\ t$	k_1 = -slope, qe = exp(intercept)	8	[21]
PFO	$q_t = q_e[1 - \exp(-k_{1p} t)]$	$\ln(q_e - q_t) = \ln q_e - k_{1p} t$	$\ln(q_e - q_t)$	$-k_{1p}$ = slope, qe = exp(intercept)	9	
Second order	$q_t = q_e/(1 + q_e k_2 t)$	$1/q_t = 1/q_e + k_2 t$	$1/q_t\ vs\ t$	k_2=slope, qe = (intercept)$^{-1}$	10	
PSO	$q_t = k_{2p} q_e^2 t/(1 + q_e k_{2p} t)$					
Type I		$t/q_t = 1/k_{2pI} q_e^2 + t/q_e$	$t/q_t\ vs\ t$	k_{2PI} = (slope)^2/intercept, qe = slope^{-1}	11	
Type II		$1/q_t = (1/k_{2pII} q_e^2)(1/t) + 1$	$1/q_t\ vs\ 1/t$	k_{2PII} = (intercept)^2/slope, qe = intercept^{-1}	12	
Type III		$q_t = q_e - (1/k_{2PIII} q_e) q_t/t$	$q_t\ vs\ q_t/t$	k_{2PIII} = -1/(slope x intercept), qe = intercept	13	
Type IV		$q_t/t = k_{2PIV} q_e^2 - k_{2PIV} q_e q_t$	$q_t/t\ vs\ q_t$	k_{2PIV} = (slope)^2/ intercept, qe = -intercept/slope	14	
Intra-particle diffusion	$q_t = k_{id} t^{1/2} + C$	$q_t = k_{id} t^{1/2} + C$	$q_t\ vs\ t^{1/2}$	C= intercept, k_{id} = slope	15	[7]

3. RESULTS AND DISCUSSION

3.1 Adsorbent Characterization

Physic-chemical and instrumental characteriza-tion results for AARHS had been presented in our earlier publication [22].

3.2 Equilibrium Isotherm Studies

The adequacy of the models in describing the equilibrium data was based on R^2, RMSE, χ^2 and ARE values. The model with R^2 closest to unity and least RMSE, χ^2 and ARE values is considered most adequate. Comparing the robustness of the linear transformations of Langmuir isotherm in capturing the equilibrium data, it was observed that the equilibrium data best followed Langmuir type I isotherm. However, Freundlich isotherm was consistently better than Langmuir type I isotherm at 303 K, 313 K and 323 K in fitting the equilibrium data thereby proposing that the remediation of CV dye aqueous solution occurred on heterogeneous AARHS surface. In addition, the best fit recorded by Freundlich isotherm model also suggests multilayer adsorption of CV dye. Freundlich's degree of nonlinearity between solution concentration and adsorption (n) describes adsorption process to be linear when n = 1; a chemical process when n < 1 and when n>1 a physical process. The calculated n values of 1.9685 (Table 4), 2.2321 (Table 5) and 1.9417 (Table 6) recorded at 303K, 313K and 323K respectively suggest adsorption of CV dye onto AARHS to be a physical process [23;24]. Also Arami et al., [25] reported that the inverse of Freundlich's isotherm parameter (1/n) indicates the type of adsorption to be irreversible when 1/n =0, favourable (0<1/n<1) and unfavourable (1/n>1). The values obtained for 1/n at all the temperatures under investigation lie between 0 and 1indicating the favourability of the adsorption process.

Figs. 1a, 1b and 1c display plots of predicted amount of CV dye adsorbed at equilibrium by Langmuir Type 1 and Freundlich isotherms against experimentally derived amount of dye adsorbed at 303 K, 313 K and 323K respectively. Predictions from Freundlich isotherm revealed minimal deviation from experimental data at all the temperatures examined compared to Langmuir Type I isotherm predictions confirming that the experimental data best followed the Freundlich isotherm.

**Table 4. Calculated isotherm for CV dye adsorption onto AARHS at 303 K**

Isotherms	R^2	RMS	χ^2	ARE(%)	Parameters
Langmuir					
Type I	0.967	0.2517	1.5539	11.2552	qm = 58.8235 mg/g; K_L = 0.0590 L/mg
Type II	0.925	0.3272	6.4988	14.6314	qm = 35.7143 mg/g; K_L = 0.1564 L/mg
Type III	0.719	0.3083	2.8128	13.7890	qm = 43.8800 mg/g; K_L = 0.1084 L/mg
Type IV	0.719	0.2984	1.6470	13.3431	qm = 51.9359 mg/g; K_L = 0.0780 L/mg
Freundlich	0.993	0.0829	0.1814	3.7697	n = 1.9685; K_F = 6.203 mg/g(L/mg)$^{1/n}$

Table 5. Calculated isotherm for CV dye adsorption onto AARHS at 313 K

Isotherms	R^2	RMS	χ^2	ARE(%)	Parameters
Langmuir					
Type I	0.964	0.3457	3.7960	15.4608	qm = 55.5556 mg/g; K_L = 0.1011 L/mg
Type II	0.856	0.3622	4.5647	16.1964	qm = 40 mg/g; K_L = 0.2033 L/mg
Type III	0.642	0.3952	4.3304	17.6720	qm = 40.71 mg/g; K_L = 0.2122 L/mg
Type IV	0.642	0.3573	3.1559	15.9794	qm = 50.2941 mg/g; K_L = 0.136 L/mg
Freundlich	0.945	0.2201	1.0789	9.8428	n = 2.2321; K_F = 8.6193 mg/g(L/mg)$^{1/n}$

Table 6. Calculated isotherm for CV dye adsorption onto AARHS at 323 K

| Isotherms	R^2	RMS	χ^2	ARE(%)	Parameters
Langmuir					
Type I	0.986	0.2254	1.0300	10.0789	qm = 62.5 mg/g; K_L = 0.0643 L/mg
Type II	0.946	0.2582	3.9165	11.5453	qm = 40 mg/g; K_L = 0.1389 L/mg
Type III	0.811	0.2294	1.4396	10.2591	qm = 48.32 mg/g; K_L = 0.1004 L/mg
Type IV	0.811	0.2166	0.8866	9.6883	qm = 54.4321 mg/g; K_L = 0.081 L/mg
Freundlich	0.987	0.1146	0.3936	5.1251	n = 1.9417; K_F = 6.5078 mg/g(L/mg)$^{1/n}$
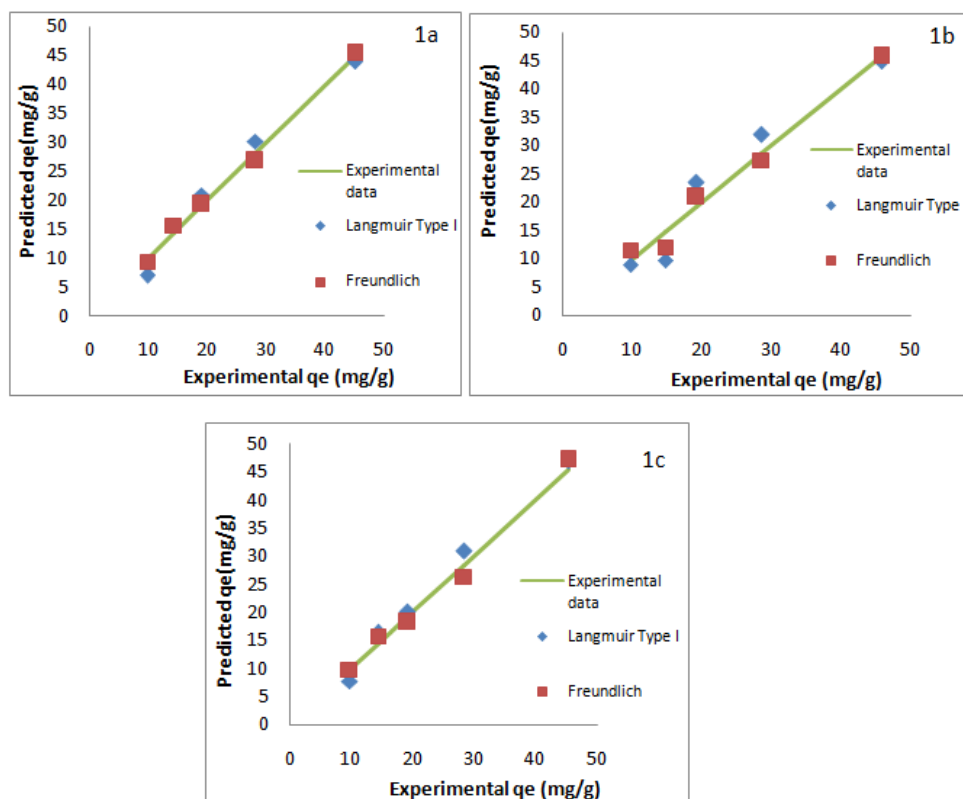
Fig. 1. Plot of predicted qe vs experimental qe at (a) 303 K (b) 313 K and (c) 323 K

3.3 Kinetics Study

The applicability of zero order, first order, pseudo-first order, second order and type I, II, III and IV pseudo-second order kinetic models were evaluated for the adsorption of CV dye onto AARHS. The efficiency of the models in describing the kinetics of the process was measured using coefficient of determination (R^2), root mean square error (RMSE), chi square (χ^2) and average relative error (ARE) values. Fig. 2 presents a plot of the amount of CV dye adsorbed (mg/g) against contact time at different temperatures (303, 313 and 323 K). It was observed that the amount of dye uptake, qt (mg/g) increased with increase in contact time at all temperatures. Also, there was an initial rapid uptake of CV dye on AARHS for the first 60 minutes after which further increase in time had milder effect on the response (qt). At this region, insignificant CV dye was removed from the solution. The observed initial rapid uptake may be as a result of relatively higher availability of adsorbent active sites.

The linear regression method of least squares was adopted to determine the parameters of the selected kinetic models. The values for the investigated models' parameters, coefficient of determination (R^2), root mean square error (RMSE), chi square (χ^2) and average relative error (ARE) at 303K, 313K and 323K were presented in Tables 7, 8 and 9. Some level of resemblance was observed in the predictions of some of the investigated models. Conventionally, lower values of error functions (RMSE, χ^2 and ARE) and higher coefficient of determination (R^2) values suggest higher capability of a model in describing the process experimental data. The high R^2 (>0.9) and low RMSE (<0.02), χ^2 (< 0.08) and ARE (<2%) values recorded by PSO type I, II and IV models suggest their better applicability in predicting the experimental kinetic data at 303 K, 313 K and 323 K compared to zero order, first order, PFO, second order and PSO Type III models. The good fit displayed by PSO type I, II and IV models in predicting the kinetic experimental data for CV dye aqueous solution remediation using AARHS as adsorbent is probably an indication that the rate of adsorption follows PSO chemisorptions mechanism. PSO model assumes that the rate of adsorption of solute is proportional to the available sites on the adsorbent. Also, the reaction rate is dependent on the amount of solute on the surface of the adsorbent [26].
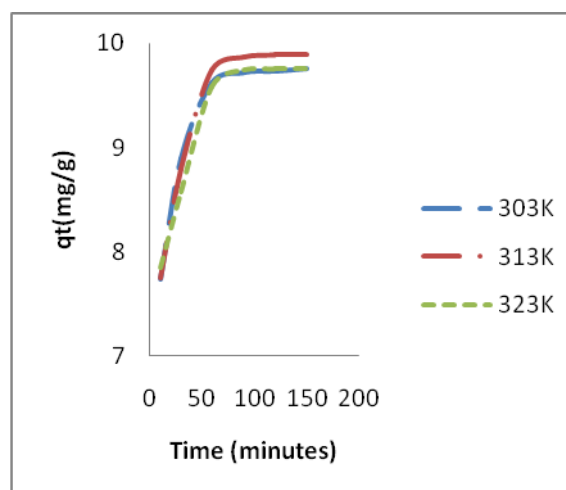
Fig. 2. Effect of contact time at different temperatures for adsorptive uptake of CV dye onto AARHS

Kinetic experimental data were also fitted into the intra-particle diffusion kinetic model to reveal the definite mechanism of the adsorption process which the earlier studied models cannot identify. The adsorption of solute in a solution involves mass transfer of adsorbate (film diffusion), surface diffusion and pore diffusion. Film diffusion is an independent step, whereas surface and pore diffusion may occur simultaneously [26]. It is assumed that the rate is not limited by mass transfer from the bulk solution to the external surface of the adsorbent due to the particles are vigorously agitated during the sorption period [12]. If the regression of q_t versus $t^{1/2}$ is linear and passes through the through the origin, then intra-particle diffusion is the sole rate-limiting step [27]. When the plots do not pass through the origin, this is indicative of some degree of boundary layer control and this further show that the intra-particle diffusion is not the only rate-limiting step, all of which may be operating simultaneously [25]. Fig. 3 presents the plot of the Weber and Morris equation (q_t versus $t^{1/2}$) for CV dye adsorption on AARHS at 313 K. It is observed from the plot that there are two separate stages. In stage I, > 70% of CV dye was speedily up taken by AARHS within 10 minutes. This may be as a result of the immediate utilization of the most readily available adsorbing sites on the adsorbent surfaces. In stage II, very slow diffusion of adsorbate from surface site into the inner pores was observed [28]. This same trend was observed at 303 K and 323 K (plots not shown).

Table 7. Calculated kinetic parameters for CV dye adsorption onto AARHS at 303 K

Kinetics models	R^2	RMSE	χ^2	ARE(%)	Parameters
Zero order	0.656	0.0713	0.3753	5.7057	qe= 7.733 mg/g; K = -0.012 mg/g.h
First order	0.640	0.2038	3.8269	17.1864	qe = 8.290 mg/g; K_1 = -0.00138 h^{-1}
PFO	0.959	0.7150	157.985	66.0350	qe = 2.609 mg/g; K_{p1} = 0.043 h^{-1}
Second order	0.624	0.0978	0.5435	6.9434	qe = 8.271 mg/g; K_2 = -0.00024 g/mg.h
PSO					
Type I	0.999	0.0111	0.0075	0.7623	qe = 10 mg/g; K_{2I} = 0.0350 g/mg.h
Type II	0.986	0.0100	0.0062	0.6596	qe =10 mg/g; K_{2II} = 0.0341 g/mg.h
Type III	0.981	0.0435	0.1277	3.9285	qe = 9.544 mg/g; K_{2III} = 0.0341 g/mg.h
Type IV	0.981	0.0097	0.0059	0.7199	qe = 10.003 mg/g; K_{2IV} = 0.0333 g/mg.h

Table 8. Calculated kinetic parameters for CV dye adsorption onto AARHS at 313 K

Kinetics models	R^2	RMS	χ^2	ARE(%)	Parameters
Zero order	0.692	0.0568	0.2829	4.5036	qe= 7.865 mg/g; K = -0.013 mg/g.h
First order	0.676	0.2148	4.7722	18.0196	qe = 8.258 mg/g; K_1 = -0.000153 h^{-1}
PFO	0.995	0.5246	44.7165	48.0905	qe = 4.735 mg/g; K_{p1} = 0.057 h^{-1}
Second order	0.663	0.0852	0.3552	6.2143	qe = 8.237 mg/g; K_2 = -0.00023 g/mg.h
PSO					
Type I	0.999	0.0181	0.0189	1.4930	qe = 10.204 mg/g; K_{2I} = 0.0294 g/mg.h
Type II	0.963	0.0131	0.0171	0.9482	qe =10.101 mg/g; K_{2II} = 0.0317 g/mg.h
Type III	0.951	0.0432	0.1800	3.8359	qe = 9.614 mg/g; K_{2III} = 0.0313 g/mg.h
Type IV	0.951	0.0568	0.0174	1.2779	qe = 10.167 mg/g; K_{2IV} = 0.0295 g/mg.h

Table 9. Calculated kinetic parameters for CV dye adsorption onto AARHS at 323 K

Kinetics models	R^2	RMS	χ^2	ARE(%)	Parameters
Zero order	0.730	0.0568	0.1833	4.5197	qe= 7.943 mg/g; K = -0.012 mg/g.h
First order	0.721	0.2102	4.0573	17.6434	qe = 8.214 mg/g; K_1 = 0.0014 h^{-1}
PFO	0.966	0.5902	66.0606	54.3002	qe = 4.003 mg/g; K_{p1} = 0.053 h^{-1}
Second order	0.710	0.0609	0.1926	4.8270	qe = 8.2034 mg/g; K_2 = -0.0002 g/mg.h
PSO					
Type I	0.999	0.0137	0.0414	1.0746	qe = 10.101 mg/g; K_{2I} = 0.0293 g/mg.h
Type II	0.915	0.0108	0.0313	0.8434	qe = 9.9010 mg/g; K_{2II} = 0.0370 g/mg.h
Type III	0.897	0.0483	0.1662	4.3923	qe = 9.452 mg/g; K_{2III} = 0.0364 g/mg.h
Type IV	0.897	0.0102	0.0332	0.8027	qe = 10 mg/g; K_{2IV} = 0.0322 g/mg.h
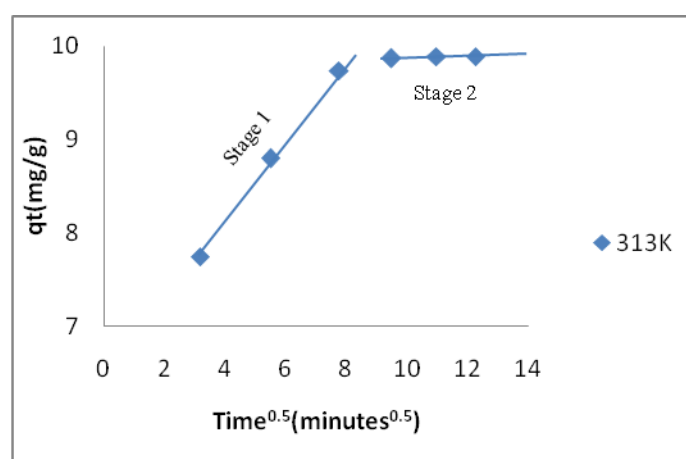
Fig. 3. Intra-particle plot of CV dye adsorption onto AARHS at 313 K

As can be seen in Fig. 3, the linear lines did not pass through the origin and this deviation from the origin indicates that intra-particle transport is not the sole rate limiting step, possibly both intra-particle diffusion and surface adsorption contribute to the rate determining step. The non-

Table 10. Calculated intra-particle diffusion parameters

Temperature	Stage 1			Stage 2		
	k_{id1}	C_1	R_1^2	k_{id2}	C_2	R_2^2
303K	0.410	6.511	0.983	0.010	9.615	0.949
313K	0.434	6.391	0.999	0.007	9.802	0.780
323K	0.377	6.609	0.990	0.007	9.671	0.998

passage of the plots through the origin may also be as a result of some degree of boundary layer control [29]. According to Bayramoglu et al. [27], the intercept (C) of the plot of qt versus time$^{1/2}$ gives an idea about boundary layer thickness, the larger the value of the intercept, the greater the boundary layer diffusion effect is. From Table 10, higher boundary layer diffusion effect was observed more at the second stage for all the temperatures (303 K, 313 K and 323 K) evaluated. The initial portion of CV dye's adsorption onto AARHS may be governed by the initial intra-particle transport of CV dye controlled by surface diffusion process and later part is controlled by pore diffusion. Similar dual nature with initial linear and then plateau were found in the literature [28;30].

4. CONCLUSION

The possibility of using an agro waste of regenerative resource as a precursor for preparation of an adsorbent for the remediation of CV dye aqueous solution was successfully demonstrated at various experimental conditions. Among all the isotherms investigated, Freundlich isotherm best fitted the equilibrium data, indicating the possibility that the adsorption process occurred on a heterogeneous surface. Calculated Freundlich's parameter indicates the favourability of the adsorption process. PSO type I, II and IV kinetic models was consistently better in predicting the kinetic data of the process. Intra-particle diffusion plots reveal that the adsorption process of CV dye onto AARHS proceeded in two stages and also, intra-particle diffusion is not the only rate-limiting step.

COMPETING INTERESTS

Authors have declared that no competing interests exist.

REFERENCES

1. Al Da'amy MA, Al Rubaeey ET, AL Khaleeli AB, Abdul Majeed MN, Al Njar ZA. Adsorption of cationic dyes from synthetic textile effluent by Iraqi porcelanite rocks. Journal of Asian Scientific Research. 2013;3(10):1011-1021.
2. Patel H, Vashi RT. Adsorption of crystal violet dye onto Tamarind seed powder. Journal of Chemistry. 2010;7(3):975-984.
3. Vijayakumar G, Tamilarasan R, Dharmendirakumar M. Adsorption, kinetic, equilibrium and thermodynamic studies on the removal of basic dye Rhodamine-B from aqueous solution by the use of natural adsorbent perlite. J. Mater. Environ. Sci. 2012;3(1):157-170.
4. Ong ST, Lee CK, Zainal Z. Removal of basic and reactive dyes using ethylenediamine modified rice hull. Bioresource Technology. 2007;98:2792-2799.
5. El Ouahabi I, Slimani R, Benkaddour S, Hiyane H, Rhallabi N, Cagnon B, El Haddad M, El Antri S, Lazar S. Adsorption of textile dye from aqueous solution onto a low cost conch shells. J. Mater. Environ. Sci. 20189(7);1987-1998.
6. Soonmin H. Removal of dye by adsorption onto activated carbons: review. Eurasian Journal of Analytical Chemistry. 2018; 13(4):332-338.
7. Bulut Y, Aydin H. A kinetics and thermodynamics study of methylene blue adsorption on wheat shells. Desalination. 2006;194:259-267.
8. Ramachandran P, Vairamuthu R, Ponnusamy S. Adsorption isotherms, kinetics, thermodynamics and desorption studies of reactive orange 16 on activated carbon derived from *Ananas cosmosus* (L.) carbon. ARPN Journal of Engineering and Applied Sciences. 2011; 6(11):15-26.
9. Chaiyaraksa C, Ruenroeng C, Buaphuan B, Choksakul S. Adsorption of cationic and anionic dye using modified pineapple peel. Songklanakarin J. Sci. Technol. 2019; 41(1):199-206.
10. Seow TW, Lim CK. Removal of dye by adsorption: A review. International Journal of Applied Engineering Research. 2016;11(4):2675-2679.

11. El-Khaiary MI. Least-squares regression of adsorption equilibrium data: comparing the options. Journal of Hazardous Materials. 2008;158(1):73–87.

12. Behnamfard A, Salarirad MM. Equilibrium and kinetic studies on free cyanide adsorption from aqueous solution by activated carbon. Journal of Hazardous Materials. 2009;170:127-133.

13. Ayawei N, Ebelegi AN, Wankasi D. Modelling and interpretation of adsorption isotherms. Journal of Chemistry; 2017. Available:https://doi.org/10.1155/2017/3039817

14. Li K, Zheng Z, Huang X, Zhao G, Feng J, Zhang J. Equilibrium, kinetic, thermodynamic studies on the adsorption of 2-nitroaniline onto activated carbon prepared from cotton stalk fibre. Journal of Hazardous Materials. 2009166:213-220.

15. Okoye CC, Onukwuli OD, Okey-Onyesolu CF. Utilization of salt activated *Raphia hookeri* seeds as biosorbent for Erythrosine B dye removal: Kinetics and thermodynamics studies. Journal of King Saud University. 2019;31:849-858.

16. Aznar SJ. Characterization of activated carbon produced from coffee residues by chemical and physical activation. Sweden: KTH Chemical Science and Engineering; 2011. Available:http://www.diva-portal.org/smash/get/diva2:414291.pdf

17. Palanivell P, Ahmed OH, Latifah O, Majid NMA. Adsorption and desorption of nitrogen, phosphorus, potassium, and soil buffering capacity following application of chicken litter biochar to an acid soil. Applied sciences. 2020;10(295): 1-18.

18. Piccin JS, Dotto GL, Pinto LAA. Adsorption isotherms and thermochemical data of FD&C red N°40 binding by chitosan. Brazilian Journal of Chemical Engineering. 2011;28(2):295–304.

19. Dada AO, Olalekan AP, Olatunya AM, Dada O. Langmuir, Freundlich, Temkin and Dubinin–Radushkevich isotherms studies of equilibrium sorption of Zn^{2+} unto phosphoric Acid modified rice husk. Journal of Applied Chemistry. 2012; 3(1):38-45.

20. Foo KY, Hameed BH. Insights into the modeling of adsorption isotherm systems. Chem. Eng. J. 2010;156:2–10.

21. Robati D. Pseudo-second-order kinetic equations for modeling adsorption systems for removal of lead ions using multi-walled carbon nanotube. Journal of Nanostructure in Chemistry. 2013;3(55):1-6.

22. Okoye CC, Onukwuli OD, Okey-Onyesolu CF. Predictive capability evaluation of RSM and ANN models in adsorptive treatment of crystal violet dye simulated wastewater using activated carbon prepared from *Raphia hookeri* seeds. Journal of the Chinese Advanced Materials Society. 2019;6(4): 478-496..

23. Ajenifuja E, Ajao JA, Ajayi EOB. Adsorption isotherm studies of Cu (II) and Co (II) in high concentration aqueous solutions on photocatalytically modified diatomaceous ceramic adsorbents. Appl Water Sci. 2017;7:3793–3801.

24. Desta MB. Batch Sorption Experiments: Langmuir and Freundlich Isotherm Studies for the Adsorption of Textile Metal Ions onto Teff Straw (*Eragrostis tef*) Agricultural Waste. Journal of Thermodynamics; 2013. Available:http://dx.doi.org/10.1155/2013/375830

25. Arami M, Limaee NY, Mahmoodi NM. Evaluation of the adsorption kinetics and equilibrium for the potential removal of acid dyes using a biosorbent. Chemical Engineering Journal. 2008;139:2-10.

26. Emik S, Öngen A, Özcan HK, Aydin S. Modelling of adsorption kinetic processes – errors, theory and application. In Edebali S (Ed.). Advanced Sorption Process Application; 2018. DOI: 10.5772/intechopen.80495

27. Bayramoglu G, Altintas B, Arica M. Adsorption kinetics and thermodynamic parameters of cationic dyes from aqueous solutions by using a new strong cation-exchange resin. Chemical Engineering Journal. 2009;152:339-346.

28. Chakrapani C, Babu CS, Vani KNK, Somasekhara RK. Adsorption kinetics for the removal of fluoride from aqueous solution by activated carbon adsorbents derived from the peels of selected citrus fruits. Journal of Chemistry. 2010;7(1):419-427.

29. Senthil KP, Senthamarai C, Durgadevia A. Adsorption kinetics, mechanism, isotherm, and thermodynamic analysis of copper ions onto the surface modified agricultural waste. Environmental Progress & Sustainable Energy. 2012; 33(1):28-37.

30. Kumar E, Bhatnagar A, Ji M, Jung W, Lee S, Kim S, Lee G, Song H, Choi J, Yang J, Jeon B. Defluoridation from aqueous solutions by granular ferric hydroxide (GFH). Water Research. 2009;43:490-498.

Peer-review history:
The peer review history for this paper can be accessed here:
http://www.sdiarticle4.com/review-history/59522